Open-State Occupancy Prevents Gating Charge Relaxation of N-type (CaV2.2) Calcium Channels

Viktor Yarotskyy[†] and Keith S. Elmslie[†‡*]
[†]Department of Anesthesiology and [‡]Department of Pharmacology, Penn State College of Medicine, Penn State University, Hershey, Pennsylvania

ABSTRACT N-type and L-type channels have significant gating differences, and we wondered whether some of these differences are linked to the relationship between charge movement and channel opening. The time constants for N-channel closing (τ_{Deact}) and Off-gating charge movement (τQ_{Off}) were compared over a range of voltages. τQ_{Off} was significantly larger than τ_{Deact} at voltages < -10 mV, and the voltage dependence of the τQ_{Off} was less steep than that for τ_{Deact}, which suggests that gating charge relaxation does not limit channel closing. Roscovitine, a drug that slows N-channel closing by holding the channel in a high open-probability state, was found to slow both τQ_{Off} and τ_{Deact}, and thus the time courses of channel closing and gating charge relaxation were similar. Our gating current results were reproduced with the addition of a voltage-independent, closed-closed transition to our previously published two-open-state N-channel model. This work suggests that, like L-type channels, there is a voltage-independent transition along the N-channel activation/deactivation pathway, but this transition occurs between closed states instead of the closed-open states of the L-channel. Also unlike L-type channels, the gating charge appears to be locked into the activated position by the N-channel open state.

INTRODUCTION

Voltage-dependent calcium channels are crucial regulators of neuronal function. However, our understanding of the fundamental gating mechanisms of these channels has lagged behind that of other voltage-dependent channels. One reason for this is the limited number of gating modifiers that exist for these channels, which is particularly true for the CaV2 class (1). Roscovitine is a cyclin-dependent kinase inhibitor that slows the closing of CaV2 channels (2–5). We were able to reproduce the effect of roscovitine on N-type calcium channels using a two-open-state gating model, with roscovitine exclusively binding to the open states and with the high open-probability (P_o) state having 20× higher affinity for roscovitine (2). Although the roscovitine-induced slowed deactivation was somewhat reminiscent of the BayK8644 effect on L-type (CaV1.2) channels, there were significant differences. First, roscovitine can only bind after the channel opens, and thus binds-unbinds with every voltage step (2), whereas BayK8644 is constantly bound to L-channels (6,7). Second, the high P_o state to which roscovitine preferentially binds is predicted to be part of normal N-channel gating (2), whereas BayK8644 shifts gating into a novel L-channel gating mode that is not typically achieved under control conditions (6,7). The effect of both BayK8644 on L-channels and roscovitine on N-channels has greatly enhanced our understanding of calcium channel gating.

Although BayK8644 induces a dramatic slowing of L-channel deactivation, its effect on gating charge movement is not so pronounced (8–10). The same BayK8644 concentration that maximally slows L-channel deactivation slows only a small fraction (~20%) of the L-channel Off-gating current (8–10), which suggests that Off-gating charge (Q_{Off}) movement may be not limited by L-channel closing. Another L-channel agonist, FPL64176, has no effect on the time course of L-channel Q_{Off} (11), which further supports the idea that charge movement can be dissociated from L-channel closing.

In an attempt to understand the fundamental properties of N-channel gating, we used roscovitine to probe the link between channel opening and gating charge movement. One clue to suggest that this relationship would differ from that of L-channels is that N-channels exhibit voltage-dependent open times (12), whereas L-channel open times have been shown to be voltage-independent (6,7). Thus, we anticipated a different relationship between channel closing and gating charge movement. We found that roscovitine significantly slowed Q_{Off} relaxation, with relatively minor affects on Q_{On} kinetics. Our results were reproduced by our gating model (described above) after significant modifications were made, including the addition of two closed states with a voltage-independent transition between them. The existence of such a transition is supported by previous single N-channel recordings (12). With this model, we were able to explain differences between the voltage-dependence of N-channel deactivation versus gating charge relaxation under control conditions, and the coalescence of these values by roscovitine. Our experimental and simulation results support the notion that voltage sensors are immobilized by the N-channel open state.

Submitted December 22, 2008, and accepted for publication August 6, 2009.

*Correspondence: kse10@psu.edu

Viktor Yarotskyy's present address is Department of Pharmacology and Physiology, University of Rochester, Rochester, NY.

Editor: Jian Yang.

0006-3495/09/11/2446/10 $2.00

doi: 10.1016/j.bpj.2009.08.014

MATERIALS AND METHODS

HEK cell transfection

We used the calcium phosphate precipitation method to transfect HEK293 cells with N-channels as previously described (13). HEK293 cells were transfected with cDNA plasmids pcDNA3 (Invitrogen, Carlsbad, CA) as follows: 11.5 μg CaV2.2$_{\text{-CFP}}$, 8.5 μg $\alpha_2\delta$, 5.5 μg β_{2a} subunits, 2.15 μg TAG. CaV2.2$_{\text{-CFP}}$ contained CFP encoding cDNA attached to the N-terminus of α_{1B} to visualize transfected cells.

Measurement of currents

Cells were voltage-clamped using the whole-cell configuration of the patch-clamp technique as previously described (1). The leak current was subtracted online using a −P/4 protocol for ionic currents and −P/8 for gating currents. All recordings were carried out at room temperature, and the holding potential was −120 mV. Gating currents were recorded using 40–60% series resistance compensation, leaving a maximum voltage-clamp error of <5 mV. There was no correlation between gating current parameters and maximum voltage error and/or series resistance.

Solutions

The internal pipette solution contained (in mM) 104 NMG-Cl, 14 creatine-PO_4, 6 $MgCl_2$, 10 NMG-HEPES, 5 Tris-ATP, 0.3 Tris-GTP, and 10 NMG-EGTA with osmolarity = 280 mOsm and pH = 7.4. The external recording solution for ionic currents contained (in mM) 5 $CaCl_2$, 145 NMG-Cl, and 10 NMG-HEPES with osmolarity = 325 mOsm and pH = 7.4. Gating currents were isolated as previously described (1) using a lanthanum and magnesium (La-Mg) external solution that contained (in mM) 0.2 $LaCl_3$, 5 $MgCl_2$, 0.1 NMG-EGTA, 145 NMG-Cl, and 10 NMG-HEPES with osmolarity = 325 mOsm and pH = 7.4. Throughout the experiments, 100 μM R-roscovitine was used to modulate both ionic and gating currents, and the control external solution contained 0.2% DMSO to control for the vehicle concentration of the roscovitine solutions. Test solutions were applied from a gravity-fed perfusion system with an exchange time of 1–2 s.

Data analysis

Data were analyzed using IgorPro (WaveMetrics, Lake Oswego, OR) running on a Macintosh computer. The voltage dependence of activation (activation I/V) was measured from ionic tail currents (averaged over 0.3 ms) at −60 mV. Tail current measurement was taken 0.3 ms into the −60 mV step to allow for voltage clamp settling. Deactivation was determined from a protocol that consisted of 10 ms steps to +60 mV, followed by 22 ms steps to tail voltages ranging from 0 to −140 mV. Ionic tail currents were fitted by a single exponential function to determine deactivation τ (τ_{Deact}). The τ_{Deact} versus voltage relationship was fit by a single exponential function to determine the τ_{Deact} voltage dependence (*Ve*). Small steady-state step/tail currents introduced by the −P/8 leak subtraction protocol were measured at the end of the step/tail and subtracted from the gating currents. The total charge moved by depolarization or repolarization (Q_{On} or Q_{Off}, respectively) was calculated by integrating gating currents over the entire voltage step. The Off-gating current τ (τQ_{Off}) was calculated as for ionic current τ_{Deact} (as described above). The magnitude of Off-gating currents was calculated by averaging 0.3 ms of current at the peak. Group data were calculated as the mean ±SD throughout the study. A paired *t*-test was used for within-cell comparisons. A one-way analysis of variance with Tukey's honestly significant difference (HSD) post hoc test was used to test for differences among three or more independent groups.

Computer simulations

Simulated currents were generated using Axovacs 3 (written by Stephen W. Jones, Case Western Reserve University, Cleveland, OH) on a Macintosh G3 computer running Virtual PC 6 (Microsoft, Seattle, WA). Voltage-dependent rate constants (k_x) in the model were calculated from

$$k_x = A_x \exp(Vz_xF/RT),$$

where A_x is the rate constant at 0 mV, z_x is the charge moved, and R, T, and F are the gas constant, absolute temperature, and Faraday's constant, respectively. Simulated currents were analyzed using IgorPro, and simulated gating currents were filtered using a digital RC filter at 2.3 kHz (R = 8.4 $M\Omega \times 0.6$, C = 15 pF) before measurement to reproduce the filtering introduced by our average uncompensated series resistance (40%) and our average cell capacitance.

Chemicals

All experiments utilized R-roscovitine from LC Labs (Woburn, MA). Dulbecco's modified Eagle's medium (DMEM)/F12, DMEM, fetal bovine serum, and 100× antibiotic/antimycotic were obtained from Invitrogen (Carlsbad, CA). Other chemicals were obtained from Sigma (St. Louis, MO).

RESULTS

Effect of roscovitine on ionic currents

Roscovitine has been shown to affect multiple gating mechanisms to either enhance or inhibit Ca^{+2} influx via N-type calcium channels (2,14). The inhibitory effect of roscovitine on step currents is caused by a negative shift in the voltage dependence of closed-state inactivation (14), which can lead to gating charge immobilization (15). However, voltage-dependent inactivation is abrogated by coexpression of the CaVβ_{2a} subunit (16), and our experiments revealed that coexpressing the β_{2a} subunit with the N-channel eliminated the inhibitory effect of roscovitine (Fig. 1, *A* and *B*). On average, the current at +10 mV (peak of the I/V) was increased 21% ± 10% (± SD) by 100 μM roscovitine (n = 15), as opposed to the inhibition we observed when these channels were expressed with CaVβ_{1b} (14). Roscovitine also induced a −10.4 ± 3.7 mV (n = 14) shift of the I/V $V_{0.5}$ (Fig. 1 *C*), which was larger than previously observed (2,3) and may result from the elimination of inhibition by coexpression of the β_{2a} subunit. The roscovitine-induced slowed deactivation was similar to what we have previously observed (2,3). We conclude that coexpression of CaVβ_{2a} permits the study of the roscovitine agonist effect without the complication of roscovitine-induced inhibition.

Roscovitine left-shifts the Q/V relationship

Given the 10 mV left-shift in the I/V relationship, we were interested in how roscovitine would affect the gating charge versus voltage (Q/V) relationship. N-channel gating current (La-Mg) activates ~20 mV negative to ionic currents (5 mM Ca^{2+}), with some slight differences between Q_{On} and Q_{Off} that we have attributed to a small ionic current contamination of Q_{Off} (1). Roscovitine induced a left-shift in the Q/V relationship with $\Delta V_{0.5} = -3.5 \pm 2.4$ mV for Q_{On} and −4.3 ± 2.6 mV for Q_{Off} (Fig. 2 *C*). No effect on the Boltzmann slope factor was observed for either Q_{On}/V or Q_{Off}/V (Fig. 2, *B*

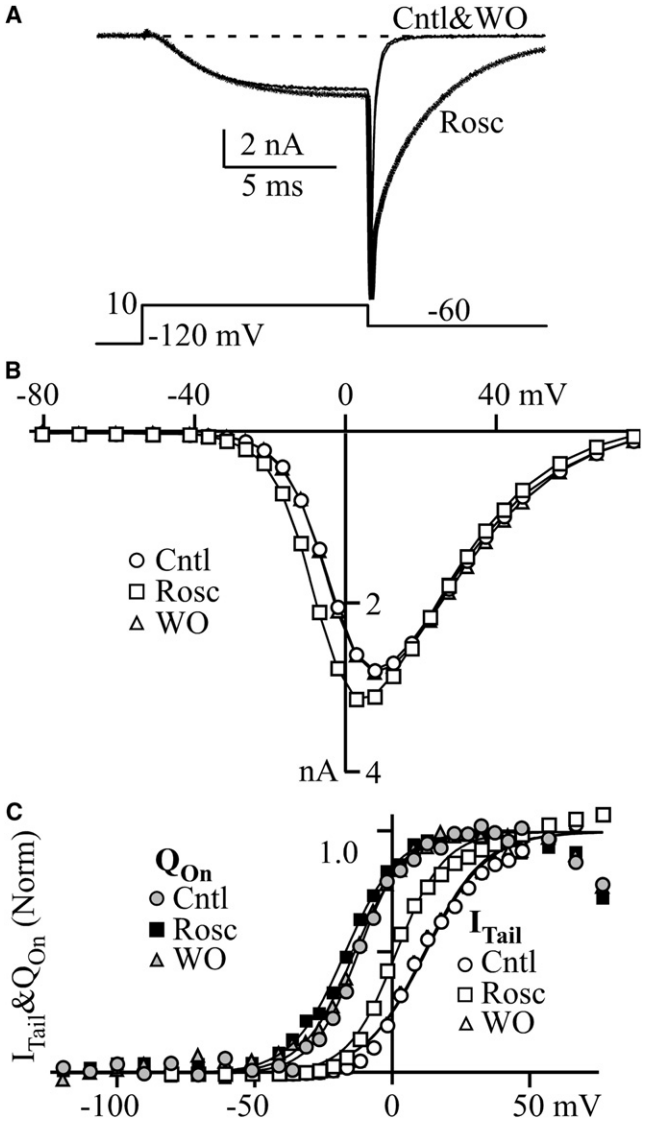

FIGURE 1 Effect of roscovitine on N-channel ionic currents. (*A*) Representative records show ionic currents in control (Cntl), 100 μM roscovitine (Rosc, *thick line*), and washout (WO). The voltage protocol is shown below. Roscovitine slightly increased the step current and dramatically slowed deactivation. (*B*) Steady-state step current (5 mM Ca^{2+}) was plotted versus voltage. (*C*) Ionic tail current (*open symbols*) and On-gating current (*solid symbols*) were plotted against step voltage and fit using a single Boltzmann equation to yield $V_{0.5}$, slope factor, and maximum current, which were used to normalize the data. The Boltzmann fitting parameters for ionic currents are (Cntl, Rosc, and WO) $V_{0.5}$ = 11.8, 1.1, and 11.2 mV; and slope factor = 11.1, 8.7, and 11.0. For On-gating currents, they are $V_{0.5}$ = −14.6, −18.6, and −15.8; and slope factor = 7.6, 8.9, and 8.6.

and *C*). We found that 100 μM roscovitine also induced a small (4.6% ± 4.5%) decrease in max Q_{On} ($n = 11$, $p < 0.01$) and a small increase in τQ_{On} at voltages < 0 mV (see Fig. 7 *F*). This increase in τQ_{On} is reminiscent of the increased N-current activation τ (τ_{Act}) observed over a similar voltage range (see Fig. 7 *E*).

The effects of roscovitine on Q_{Off} were much more dramatic, including a slowing of Q_{Off} relaxation, a decrease

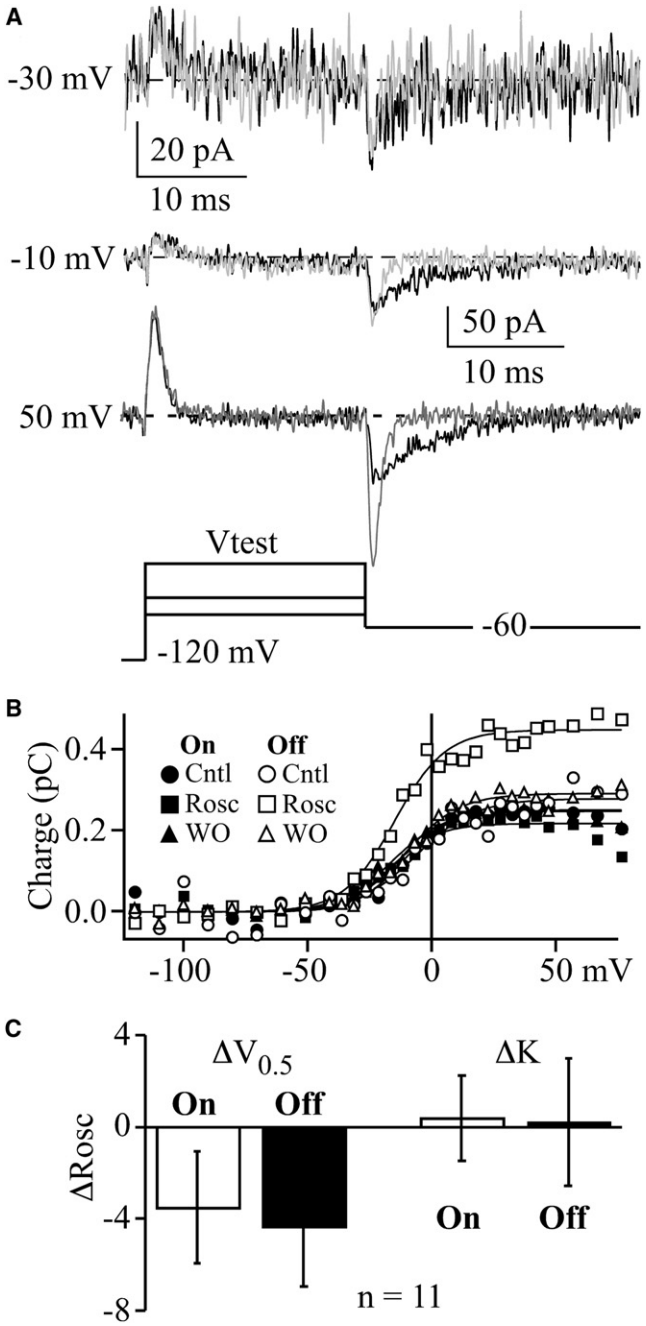

FIGURE 2 Effect of roscovitine on the Q/V relationship. (*A*) Typical traces show the voltage dependence of gating currents recorded in La-Mg; 100 μM roscovitine (*black traces*) slowed deactivation of Off-gating currents compared to control (*gray traces*) at step voltages depolarized to −20 mV. (*B*) The effect of Rosc (*squares*) on Q_{On}/V (On, *solid symbols*) and Q_{Off}/V (Off, *open symbols*) compared to Cntl (*circles*) and WO (*triangles*). The data were fitted by a single Boltzmann function (*smooth lines*) to yield (Cntl, Rosc, WO) Q_{On} $V_{0.5}$ = −12.3, −17.1 and −16.2 mV; slope factor = 9.3, 9.6, and 10.9; Q_{max} = 0.25, 0.22, and 0.25 pC; and Q_{Off} $V_{0.5}$ = −6.5, −15.3, and −10.9 mV; slope factor = 12.0, 10.3; and 10.9, Q_{max} = 0.28, 0.45, and 0.29 pC. (*C*) Roscovitine-induced changes (ΔRosc) in $V_{0.5}$ ($\Delta V_{0.5}$) and slope factor (ΔK) are not significantly different ($n = 11$) between Q_{On} (*white bars*) and Q_{Off} (*black bars*).

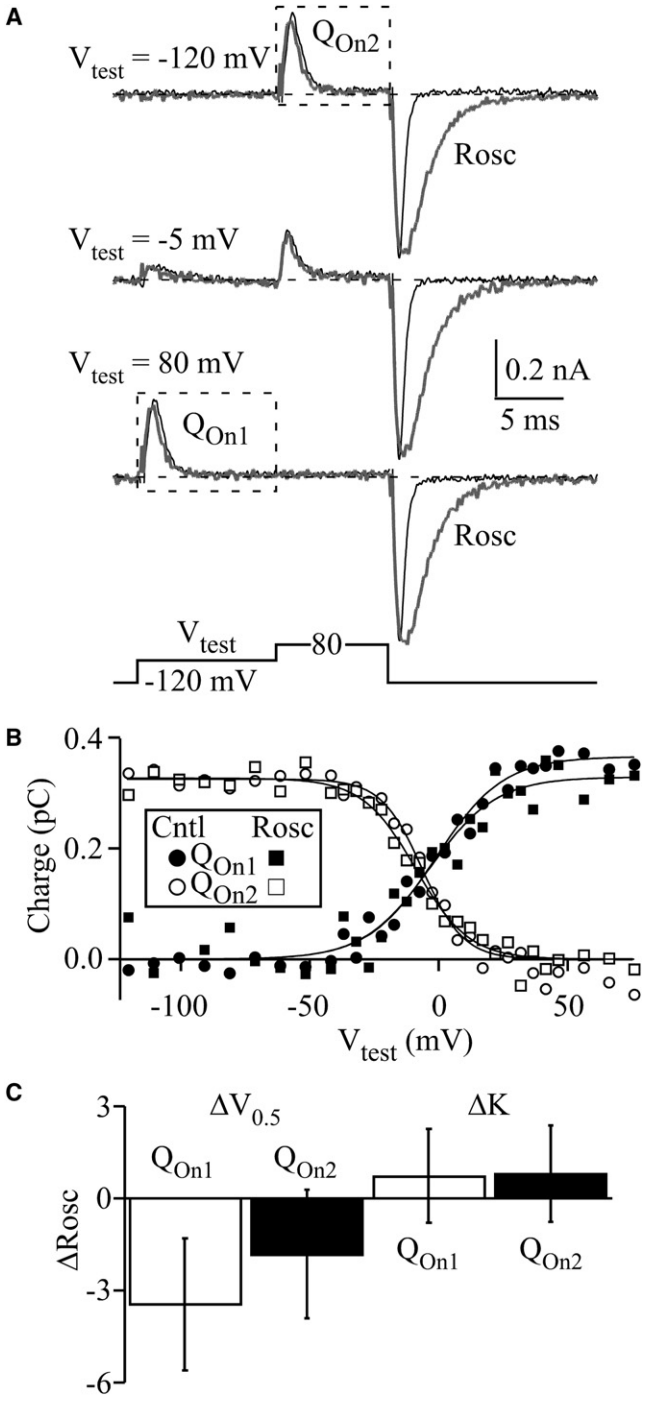

FIGURE 3 Roscovitine left-shifts the Q/V relationship. (*A*) Typical gating currents obtained from two consecutive depolarizing steps in control (*thin line*) and 100 μM roscovitine (Rosc, *thick line*). Currents are shown for three step voltages (V_{test} = −120 mV (*top*), −5 mV (*middle*), and 80 mV (*bottom*)). The second step voltage was always 80 mV. Q_{On1} and Q_{On2} are marked and represent On-gating charge movement during the first and second steps, respectively. (*B*) Q_{On1} (*solid symbols*) and Q_{On2} (*open symbols*) are plotted against V_{test} for control (Cntl, *circle*) and 100 μM roscovitine (*square*). The data are fitted by single Boltzmann functions (*smooth curves*) with parameters for Q_{On1} (Cntl and Rosc) of $V_{0.5}$ = −1 and −4 mV, and slope factor = 13 and 13. Parameters for Q_{On2} (Cntl and Rosc) were $V_{0.5}$ = −6 and −9 mV, and slope factor = 8 and 11. (*C*) The mean difference (± SD) in $V_{0.5}$ ($\Delta V_{0.5}$) and slope factor (ΔK) induced by roscovitine for Q_{On1} (*open bars*) and Q_{On2} (*solid bars*).

in peak Off-gating current (I_{Off}), and a significant increase in the apparent max Q_{Off} (Fig. 2). The slowed Q_{Off} relaxation suggests that roscovitine similarly affects gating charge movement and deactivation. The reduced peak I_{Off} is consistent with the slowed Q_{Off}, since a given amount of charge that is moved over a longer time will result in a smaller peak I_{Off}. However, the large roscovitine-induced increase in max Q_{Off} (integrated Off-gating current) was unexpected. On average, this increase was 73% ± 28% (n = 11) at −60 mV. One likely possibility is that the combination of a slowed channel closing with the strong driving force at −60 mV generated a significant ionic flux during our measurement of Q_{Off} in roscovitine.

We (1) and others (17) previously concluded that Q_{On} appears to be less contaminated by ionic current, and we used a two-pulse Q/V protocol (11) to determine the validity of the $\Delta V_{0.5}$ measured from Q_{Off}. This protocol measures the Q/V relationship as the reduction of Q_{On} at +80 mV after 10 ms steps to voltages ranging from −120 to +80 mV (Fig. 3). The advantages of this protocol are that roscovitine will have 10 ms to bind (as for the Q_{Off} measurements), and ionic current contamination will be minimal at +80 mV. As depicted in Fig. 3 *A*, Q_{On1} is equivalent to Q_{On} of the standard protocol (Fig. 2), whereas Q_{On2} is measured during the subsequent step to +80 mV. We found no significant difference between $V_{0.5}$ and slope factor in control, with $V_{0.5}$ = −6 ± 3 mV and −8 ± 8 mV, and slope = 11 ± 2 and 10 ± 3 for Q_{On1} and Q_{On2}, respectively (n = 7). Consistent with the results shown in Fig. 2, 100 μM roscovitine significantly left-shifted the $V_{0.5}$ for both Q_{On1} and Q_{On2}, with no change in the Boltzmann slope factor (Fig. 3 *C*). Thus, roscovitine left-shifts the Q/V relationship (2–5 mV), but this shift is smaller than that for ionic currents (10 mV).

Roscovitine inhibits the peak Off-gating current

The apparent ionic current contamination did not significantly impact the effect of roscovitine on the Q/V relationship, but this contamination could mediate the slowing of Q_{Off}. One possibility is that this slowing results entirely from a roscovitine-induced increase in contaminating ionic current, with no effect on the gating current. However, the Q_{Off} relaxation was best fit by a single exponential function in 100 μM roscovitine (see Fig. 5 *B*), which suggests that if two components existed, they decayed with a similar τ. In addition, if roscovitine increased ionic current contamination without an effect on Q_{Off}, we would expect to observe an increase in peak I_{Off} instead of the observed inhibition (Fig. 2 *A*). This inhibition of peak I_{Off} is expected from roscovitine-induced slowed Q_{Off}, since the same amount of gating charge is moving as in the control, but over a longer time. Thus, the reduction of

peak I_{Off} is consistent with a roscovitine-induced slowing of Q_{Off}.

Of interest, the currents in Fig. 2 *A* reveal that the roscovitine-induced reduction in peak I_{Off} is voltage-dependent and correlated with the slowing of Q_{Off}. We examined this further by measuring peak I_{Off} at −60 mV (from the Q/V protocol) in control (I_{Cntl}) versus roscovitine (I_{Rosc}) along with τQ_{Off}. The τQ_{Off} versus voltage relationship showed an increase with voltage, as would be expected if roscovitine binding were limited by low P_o at negative voltages (Fig. 4, *A* and *B*). This change was mirrored by the I_{Rosc}/I_{Cntl} ratio versus voltage relationship (Fig. 4 *C*), which was fit using a single Boltzmann equation to quantify $V_{0.5} = -18$ mV (slope factor = e-fold for −9 mV). The negative $V_{0.5}$ suggests that significant gating current modulation can occur at voltages with relatively low P_o. This along with the strong correlation between slowed Q_{Off} and inhibited I_{Off} supports the conclusion that gating current relaxation is slowed by roscovitine.

Similar deactivation and Off-gating current time courses in roscovitine

As we demonstrated previously (2), roscovitine slows ionic current deactivation at all voltages, which is accompanied by a decreased voltage dependence (*Ve*) of deactivation τ (τ_{Deact}) (Fig. 5). We therefore investigated the τQ_{Off} *Ve* to obtain a better understanding of the relationship between τQ_{Off} and τ_{Deact}. As noted above, τQ_{Off} was determined by single exponential fitting (Fig. 5 *B*). Under control conditions, τQ_{Off} was larger than τ_{Deact}, which suggests that channel closing is not limited by charge movement. Roscovitine slowed the Q_{Off} kinetics such that τQ_{Off} was nearly identical to τ_{Deact} over all voltages examined (Fig. 5 *C*). However, there was a trend for τQ_{Off} to be larger than τ_{Deact} at voltages < -90 mV, which resulted in a larger *Ve* for τQ_{Off} versus τ_{Deact} in roscovitine (Fig. 5 *D*). The correspondence between τQ_{Off} and τ_{Deact} suggests that charge movement becomes tightly coupled to channel closing in roscovitine.

Our initial analysis of Q_{Off} in roscovitine (Fig. 2) revealed significant ionic current contamination, which could explain the similar τQ_{Off} and τ_{Deact} values. If Q_{Off} is slowed by roscovitine, we should be able to observe this as a slowed recovery of Q_{On} at +60 mV (Q_{On2}) after a strong depolarization (Q_{On1}) (Fig. 6). The depolarization to the apparent reversal potential (+60 mV for La-Mg) would limit ionic current contamination for better gating current isolation. A plot of Q_{On2} versus the time interval between pulses (Fig. 6 *C*) was fit by a single exponential function to determine τQ_{On2} at interval voltages of −40 mV, −60 mV, and −80 mV. τQ_{On2} closely corresponded with τQ_{Off}, such that the values were superimposed for each voltage in both control and roscovitine (Fig. 6 *D*). We conclude that roscovitine slows channel closing and thus becomes rate-limiting to gating charge relaxation.

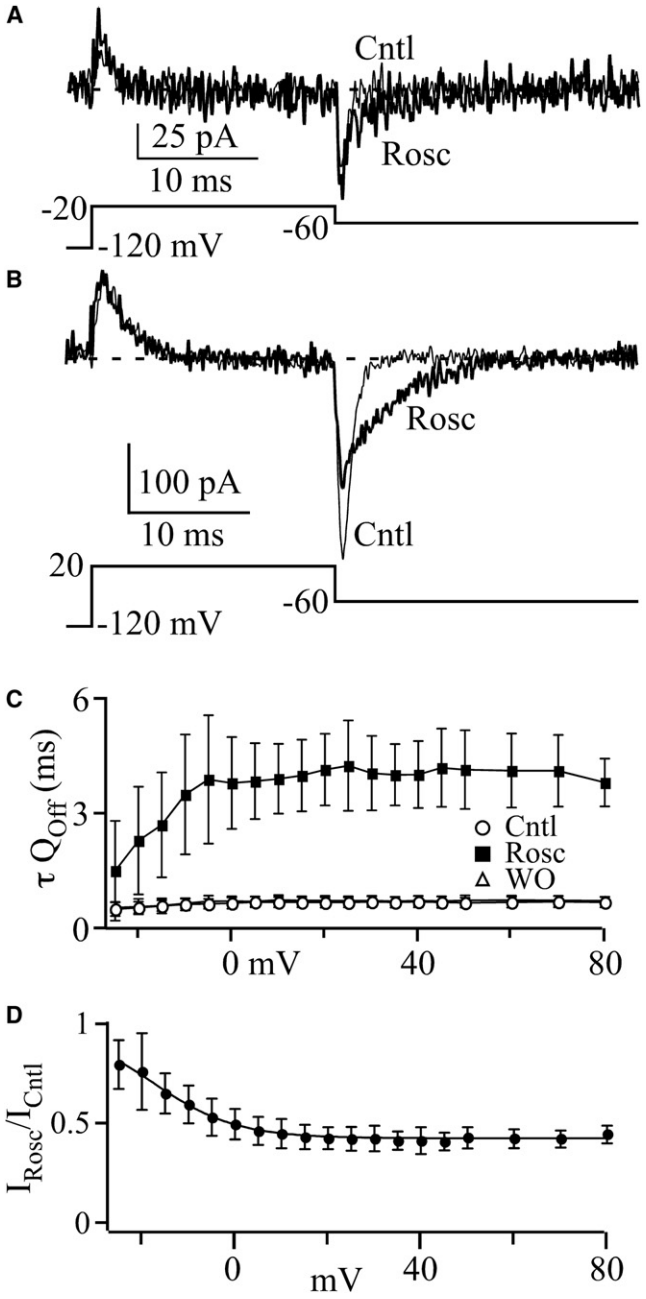

FIGURE 4 Effect of roscovitine on the kinetics and magnitude of Off-gating currents. (*A* and *B*) Representative gating current traces in Cntl (*thin line*) and 100 μM Rosc (*thick line*) are shown for −20 mV (*A*) and +20 mV (*B*) step voltages. (*C*) τQ_{Off} is plotted versus step voltage from Cntl (*open circles*), Rosc (*solid squares*), and WO (*open triangles*) ($n = 10$). (*D*) I_{Rosc}/I_{Cntl} is plotted versus step voltage to show the voltage-dependent decrease of I_{Off} in Rosc ($n = 10$). I_{Cntl} is the peak I_{Off} averaged from Cntl and WO, and I_{Rosc} is the peak I_{Off} measured in the presence of 100 μM Rosc.

N-channel model

Our experimental results support the hypothesis that roscovitine stabilizes a high P_o state to prevent gating charge

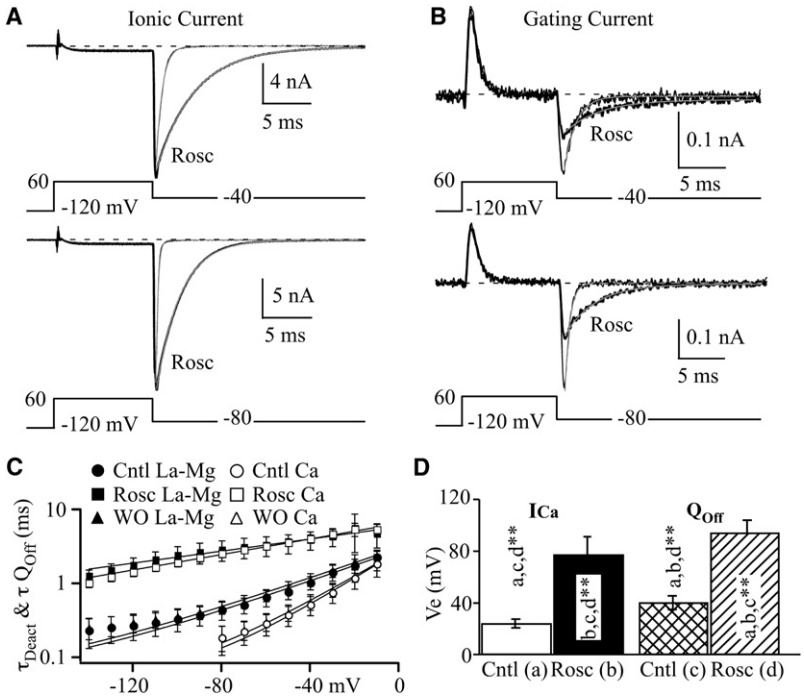

FIGURE 5 Effect of roscovitine on Off-gating current relaxation. (*A* and *B*) Typical ionic (*A*) and gating (*B*) current traces recorded in Cntl (*thin line*) and Rosc (*thick line*) at −40 mV and −80 mV tail voltages. The smooth gray lines superimposed on the tail and Q_{Off} currents are from a single exponential fit to those currents. (*C*) Ionic tail current τ_{Deact} (*open symbols*, $n = 12$) and τQ_{Off} (*solid symbols*, $n = 11$) were calculated by single exponential fitting (see panel *A*) and are plotted versus tail voltage for Cntl (*circles*), Rosc (*squares*), and WO (*triangles*). The smooth lines show the single exponential fitting to yield *Ve*. (*D*) The bar graphs show the mean *Ve* (± SD) for τ_{Deact} (ICa) and τQ_{Off} (Q_{Off}). The significant differences for all comparisons were determined using analysis of variance with Tukey's HSD post hoc test (**$p < 0.01$). The lowercase letters above each column indicate significant differences ($n = 11$).

relaxation. We tested this hypothesis using our previously published seven-state model (Scheme 1) (2):

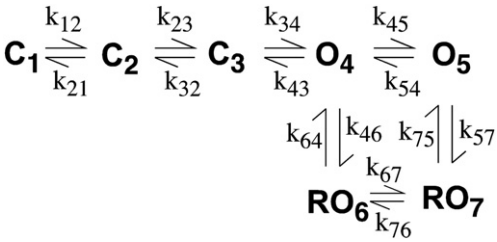

However, this model was only able to qualitatively reproduce our gating current results. For control simulations with Scheme 1, the Q/V relationship was left-shifted relative to the I/V relationship, but only by 10 mV (as opposed to the 20 mV observed in our recordings), and although τQ_{Off} was larger than τ_{Deact}, the τQ_{Off} *Ve* and τ_{Deact} *Ve* were similar (1). For the roscovitine simulations, the Q_{Off} kinetics were dramatically slowed, such that τQ_{Off} was nearly identical to τ_{Deact}, but in general, all model kinetic parameters were too fast compared to our experimental results. Although manipulation of the model parameters could overcome some of these problems, the 20 mV shift between the control Q/V and I/V relationships was difficult to obtain, and the control τ_{Deact} *Ve* and τQ_{Off} *Ve* were always similar. One clue as to how to address these issues came from the apparent plateau of control τQ_{Off} at voltages < -80 mV, which suggested a voltage-independent step within the activation/deactivation pathway. The addition of a voltage-independent transition between C_4 and C_5 (Fig. 7 *A*) lowered the control τQ_{Off} voltage dependence without affecting the τ_{Deact} *Ve* and provided excellent correspondence with our experimental results (Fig. 7 *D*). We addressed the 20 mV shift in the control Q/V versus I/V relationships by adding two additional closed states and increasing the charge moved by voltage-dependent closed-closed transitions from 0.8–0.9 (Scheme 1) (2) to 1 (*Scheme 2*, Fig. 7). Since the open states in these models are voltage-dependent, a large fraction of charge was moved by these transitions in Scheme 1 (three closed states versus two open states), which severely limited the magnitude of the achievable shift between the Q/V and I/V relationships. With the additional closed states and increased charge (*Scheme 2*, Fig. 7), we were able to achieve excellent correspondence with our control experimental Q/V relationship (Fig. 7 *C*). We also were able to nicely reproduce the control τ_{Act} versus voltage relationship (Fig. 7 *E*) and obtain decent correspondence with the τQ_{On} versus voltage relationship (Fig. 7 *F*).

The addition of 100 μM roscovitine to Scheme 2 in Fig. 7 induced a ~10 mV left-shift in the I/V relationship and a much smaller shift in the Q/V relationship, nicely reproducing our experimental results (Fig. 7 *C*). The simulated τ_{Deact} and τQ_{Off} were similar in roscovitine, but both were slightly lower than our experimental values (Fig. 7 *D*). We were able to increase these values, but that introduced an unacceptably slow activation of ionic currents and yielded τ_{Act} values in roscovitine that were too large. Thus, we compromised to achieve good correspondence of both τ_{Act} (Fig. 7 *E*) and τ_{Deact} with our experimental data. We also found a small roscovitine-induced increase in τQ_{On} at voltages near zero, but this increase was not as large as that in our experimental data (Fig. 7 *F*). Finally, we observed a voltage-dependent increase in τQ_{Off} (at −40 mV) and decrease of peak I_{Off}

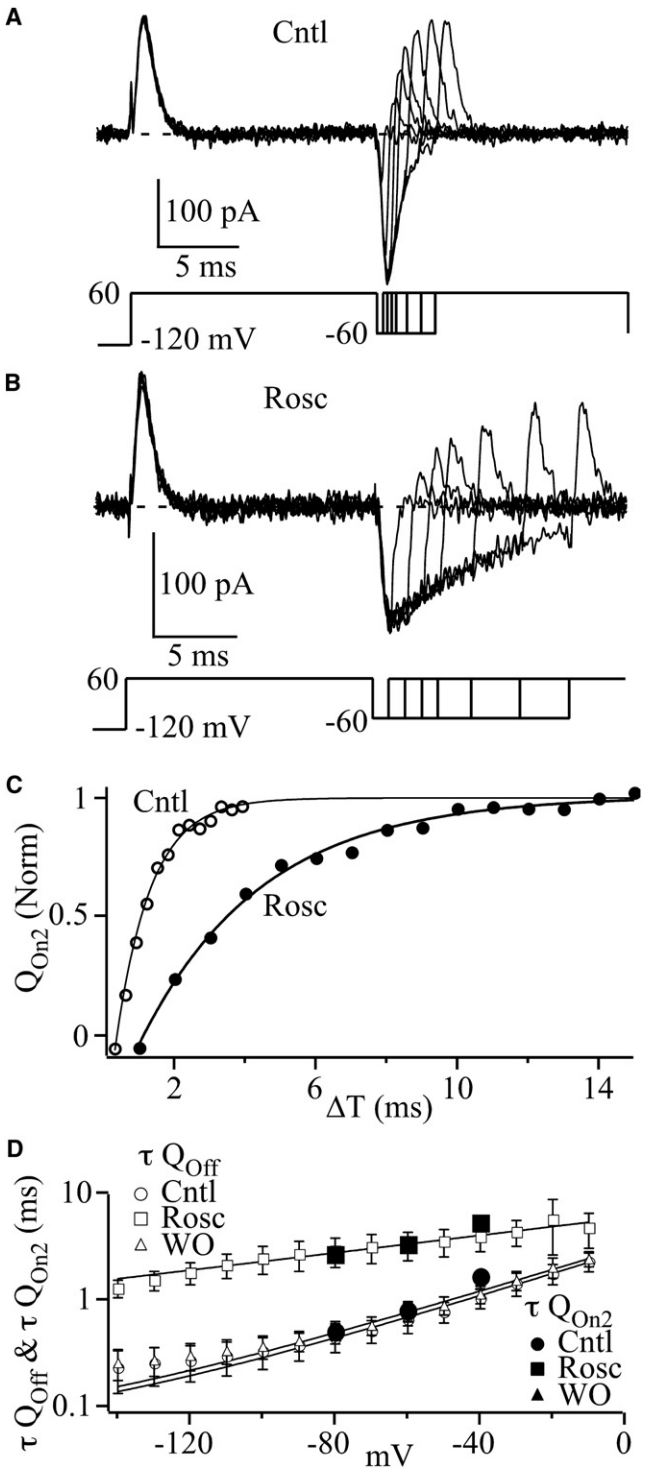

FIGURE 6 Roscovitine slows Q_{On2} recovery. (*A* and *B*) Typical traces show Q_{On2} recovery with increasing time interval between Q_{On1} and Q_{On2} in Cntl (*A*) and 100 μM Rosc (*B*). The voltage protocols are shown at the bottom. (*C*) Q_{On2} is plotted versus the interval between Q_{On1} and Q_{On2} (ΔT) to show the Q_{On2} recovery time course in Cntl (*open circle*) and Rosc (*solid circles*). The interval (tail) voltage was −60 mV, and these data are from the same cell shown in panels *A* and *B*. The recovery time course was fitted by a single exponential function to yield τQ_{On2}. (*D*) Averaged τQ_{On2} data (*solid symbols*) are superimposed with τQ_{Off} (*open symbols*) from Fig. 5 *C*. Data are shown for Cntl (*circle*), Rosc (*squares*), and WO (*triangles*). All results are shown as mean ± SD. Number of cells tested for τQ_{On2}: $n = 3$–8.

(Fig. 7, *G* and *H*) in roscovitine, which were similar to our experimental results. The revised model reproduces N-channel ionic and gating currents under control conditions, and all elements of the roscovitine effect on these currents, fully supporting our conclusion that gating charge cannot move until the channel exits the high P_o state.

DISCUSSION

Our fundamental finding is that roscovitine slows Off-gating charge movement of N-type channels, with only minor effects on On-charge movement. We conclude that roscovitine unbinding is a rate-limiting step for Off-gating current relaxation, and that the gating charge is immobilized by N-channel occupancy of the high P_o state.

Gating current isolation

Our group (1) and the Yue laboratory (17,18) previously demonstrated that Mg^{2+} and a free La^{3+} concentration of 100 μM (200 μM La^{3+} and 100 μM EGTA) generated good gating current isolation. One benefit of La-Mg is that the Q/V relationship is not affected by an equimolar exchange between Ca^{+2} and Mg^{2+} (17,18), which suggests that these two divalent cations have a similar effect on the N-channel response to membrane surface charge (19). Thus, the voltage dependence of charge movement recorded in La-Mg is directly comparable to the voltage-dependent activation of ionic currents recorded in Ca^{2+} (1,17,18). Although the La-Mg method of gating current isolation was not perfect, we found that the contaminating ionic current under control conditions was generally small and manageable (1). In roscovitine, however, ionic current contamination appeared to be a larger problem, which likely resulted from the slowed channel closing (2) that allowed significant ion conductance at the hyperpolarized potentials used to measure Q_{Off}. This contamination was observed as an increase in max Q_{Off} that likely resulted from Mg^{2+} permeation. Inorganic calcium channel blockers have been shown to permeate calcium channels at potentials where the driving force is large (20), and we have found obvious Mg^{2+} permeation via expressed N-channels ($\beta_{2a} + \alpha_2\delta$) in preliminary experiments. The 100 μM free La^{3+} in our gating current solutions normally blocks Mg^{2+} permeation, but that block is apparently partially cleared from the channel at hyperpolarized voltages (20). However, the key findings of our work that depend on Q_{Off} were verified by additional experiments that examined the roscovitine effect on Q_{On} after a preceding voltage step. In addition, our simulation results further support the roscovitine-induced effects on gating charge movement.

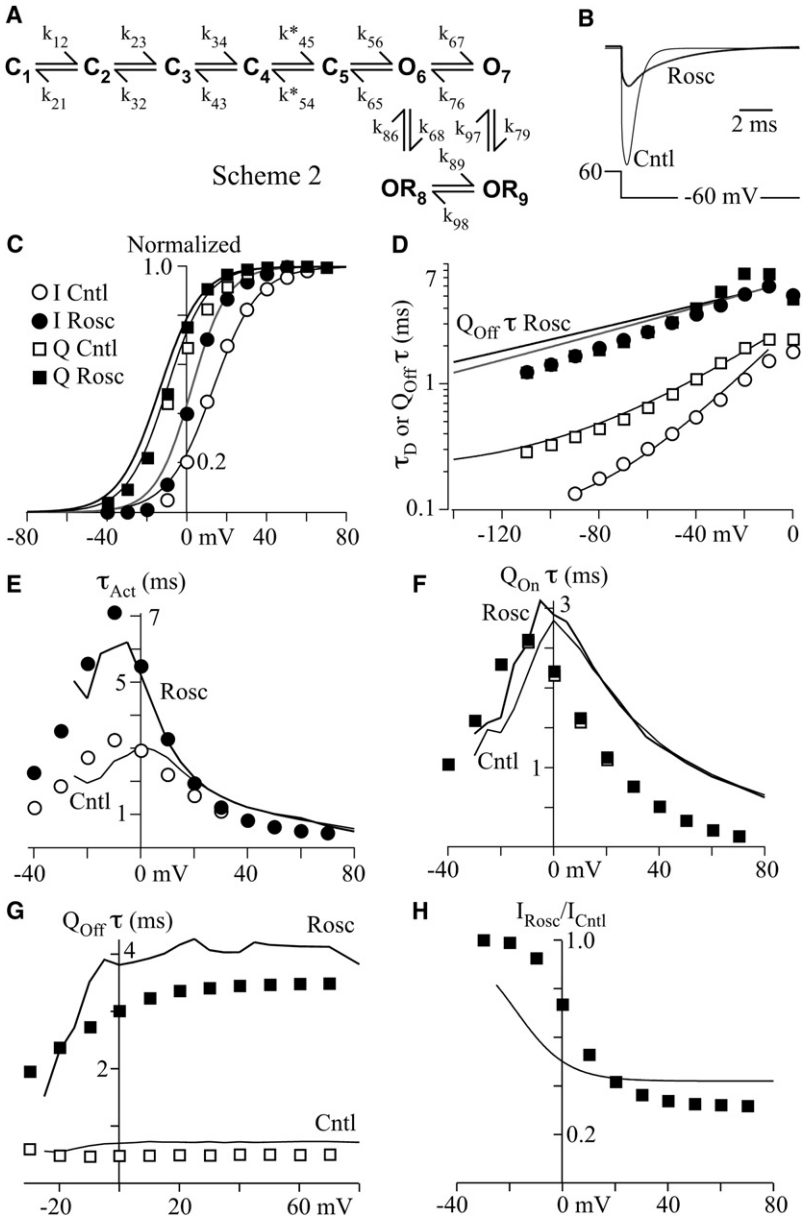

FIGURE 7 N-channel gating model reproduces the effect of roscovitine on both ionic and gating current. (*A*) The model (Scheme 2) for these simulations (see Table 1 for transition rates and charge moved). The asterisk by k45 and k54 indicates the voltage-independent transition. (*B*) Gating currents at −60 mV after a 10-ms step to +60 mV were simulated by running the model with (Rosc) and without (Cntl) 100 μM roscovitine. (*C*) A comparison of the I/V and Q_{On}/V relationships for simulations with (*solid symbols*) and without (*open symbols*) Rosc. The I/V (*circles*) and Q_{On}/V (*squares*) data were measured during repolarization to −40 mV after 15-ms steps to the voltages indicated on the *x*-axis. The symbols have the same meaning in panels *D–G*. The smooth curves are Boltzmann fits to the normalized experimental data averaged from 11 cells for the Cntl I/V, Rosc I/V, Cntl Q_{On}/V and Rosc Q_{On}/V. (*D*) Simulated ionic current τ_{Deact} (*circles*) and gating current τQ_{Off} (*squares*) are plotted versus repolarization voltage. Currents were activated by a 10 ms step to +60 mV and measured at the voltage indicated on the *x*-axis. The smooth lines are single exponential fits to the experimental data from Fig. 5 *C*. (*E*) τ_{Act} was determined by single exponential fitting of the activation phase of ionic current from the same protocol used to generate the I/V relationship (*C*) and is plotted versus step voltage. The thin line represents τ_{Act} measured from experimental data in Cntl and Rosc. (*F*) τQ_{On} was determined by single exponential fitting of the decay phase of simulated On-gating current from the same protocol used to generate the Q/V relationship (*C*) and is plotted versus step voltage. The thin line represents τQ_{On} measured from experimental data in Cntl and Rosc. (*G*) τQ_{Off} was measured from the same protocol used to generate the Q/V relationship and is plotted versus step voltage. The thin line represents the experimental data shown in Fig. 4 *C*. (*H*) Peak Off-gating current was measured from simulated gating current with (I_{Rosc}) or without (I_{Cntl}) roscovitine at −40 mV after voltage steps ranging from −40 to +70 mV (the same protocol as in panel *C*). The I_{Rosc}/I_{Cntl} ratio is plotted versus step voltage. The smooth line is the single Boltzmann equation fit to the experimental I_{Rosc}/I_{Cntl} versus voltage data from Fig. 4 *D*.

Voltage-independent transition in the activation/deactivation pathway

The addition of a voltage-independent transition to our model allowed us to reproduce our experimental ionic and gating current results. By placing this transition between closed states, we exerted little or no effect on the simulated ionic currents, but we found it possible to model the lower τQ_{Off} voltage dependence relative to that of τ_{Deact} in control. The inclusion of this transition is supported by our observation that τQ_{Off} appears to approach an asymptote at voltages < -80 mV, which suggests a voltage-independent rate-limiting step. The voltage-independent transition must be between closed states, since we have never observed a plateau for τ_{Deact} at negative voltages, which suggests that this transition does not limit channel closing. In addition, single N-channel recordings revealed voltage-dependent open times that strongly support voltage-dependent open states (12). However, the voltage-independent transition must be near the open state, since the majority of gating charge movement is limited by this transition. This location is also supported by single-channel recordings that revealed a voltage-independent closed time that became more prominent with depolarization and was concluded to represent a voltage-independent closed state near the open state (12). A potential physiological consequence is that action potential-induced N-channel opening could be delayed by the voltage-independent step until the membrane voltage repolarizes into a range in which the driving force is sufficiently strong to efficiently move

TABLE 1 Rate parameters for the N-channel model (Scheme 2 in Fig. 7)

	A	z
k12	800	1
k21	200	−1
k23	2200	1
k32	800	−1
k34	2500	1
k43	2000	−1
k45	3000	
k54	5000	
k56	1800	0.8
k65	2000	−0.8
k67	1100	0.6
k76	900	−0.6
k68	4[R]	
k86	2000	
k79	4[R]	
k97	150	
k89	1000	0.6
k98	61.37	−0.6

A (s^{-1}) is the rate constant at 0 mV, z is the charge moved, and [R] is the roscovitine concentration (μM). The units of A for k68 and k79 are $\mu M^{-1}s^{-1}$.

Ca^{+2} into the neuron to trigger neurotransmitter release and activate intracellular signaling pathways (21).

Roscovitine affects the voltage dependence of gating currents

Roscovitine left-shifts the I/V relationship, which we previously attributed to a mass-action effect of the channel being ''locked'' in the open state once roscovitine has bound (2). At voltages where the channels have an intermediate P_o, roscovitine will increase the fraction of open channels by ''trapping'' them in an open state from which exit is slow. This results in an increase in current at intermediate voltages, with little or no effect on current amplitude at strong depolarizations where P_o is maximal (Fig. 1). This same open-state trapping mechanism likely explains the roscovitine-induced small left-shift of the Q/V relationship and the increase of τQ_{On} at voltages near 0 mV, which is reminiscent of the effect of roscovitine on the N-current τ_{Act} (2). We verified this small roscovitine-induced left-shift in the Q_{Off}/V relationship using our Q_{On1}-Q_{On2} protocol, and the model nicely reproduced the small shift.

The model also reproduced the voltage-dependent effect of roscovitine to increase τQ_{Off} and decrease peak I_{Off}. Roscovitine has little effect on these parameters at hyperpolarized voltages where P_o is low, and the effect increases with depolarization. There was a strong correlation between the roscovitine-induced change in τQ_{Off} and I_{Off}, indicating that the two were linked as expected. We conclude that the inhibition of I_{Off} results from the slowing of Q_{Off} relaxation so that the same charge movement is spread over a larger area (thus the smaller I_{Off}), and this conclusion is strongly supported by our model.

N-channels closing limits Off-gating current relaxation

Under control conditions, τQ_{Off} was larger than τ_{Deact} indicating that channel closing is not limited by gating charge movement. However, in the control, it was more difficult to determine whether the opposite was true. Our model shows that the gating charge is immobilized as long as the channel is in the high P_o state. However, under control conditions, the transition out of this state is sufficiently fast that τQ_{Off} is not obviously impacted. One clue to suggest that charge movement is linked to channel closing is that in our experimental data, control τ_{Deact} and τQ_{Off} were similar at −10 mV, where deactivation may be slow enough (τ_{Deact} ~ 1 ms) to impact gating current relaxation (Fig. 5 *C*). This link was further supported by roscovitine, which sufficiently slowed channel closing so that τ_{Deact} and τQ_{Off} were similar at all deactivation voltages. In our model, movement out of the roscovitine-bound high P_o state (RO_9) occurs via both the voltage-dependent $RO_9 \rightarrow RO_8$ transition and the roscovitine-unbinding $RO_9 \rightarrow O_7$ transition, with the $RO_9 \rightarrow RO_8$ transition dominating at negative voltages. These transitions are sufficiently slow to limit both τ_{Deact} and τQ_{Off} so that the two processes have similar values. It is important to note that in our experimental data, τ_{Deact} in roscovitine was >1 ms at all voltages examined, which was the value showing correspondence between τQ_{Off} and τ_{Deact} in control (−10 mV). Thus, we believe that voltage sensor immobilization is tied to the open state, and not roscovitine binding/unbinding per se. We conclude that the N-channel must exit the high P_o state before the gating charge can relax back to the resting state.

We do not yet know where roscovitine binds to achieve its effect on deactivation, but the binding site appears to play a critical role in controlling the N-channel open state. The L-channel agonist BayK8644 binds to a site comprised of amino acids in domains III and IV, and the site appears to be accessible via the membrane (22,23). We have argued that the roscovitine-binding site is directly accessible to the extracellular solution, and this conclusion is consistent with all our available data (2,3). Thus, roscovitine likely binds to a unique, extracellularly exposed site on the N-channel to slow deactivation and voltage sensor relaxation.

The effect on the N-channel gating charge movement appears to distinguish roscovitine from the L-channel agonists BayK8644 and FPL64176, which dramatically slow L-channel closing but have a relatively minimal impact on Q_{Off} kinetics (8–11). Indeed, FPL64176 has no detectable effect on the speed of Q_{Off} (9,11). Therefore, L-channels can remain open even after the voltage sensors return to the resting state (8,9,11). FPL64176 mechanism has been proposed to involve a novel conducting state that permits voltage sensor relaxation without channel closing (11). The mechanism by which BayK8644 dissociates charge movement from channel closing is unknown, but it is possible

that this is a fundamental L-channel property. The Monod-Wyman-Changeuax model for L-channel gating predicts voltage sensor relaxation from open L-channels (7). Thus, BayK8644 and roscovitine can be used as tools to probe the fundamental relationships between charge movement and channel opening/closing, and to reveal the unique properties of these two closely related calcium channels. It is possible that this voltage sensor relaxation is linked to another difference between these two channels, which is that the L-channel open state is voltage-independent (6,7), whereas N-channels show voltage-dependent open times (12). The activated confirmation of the L-channel may dissociate open-closed gating from charge movement, whereas the activated N-channel confirmation seem to be linked to charge movement so that some charge movement is required for open-open transitions and no voltage sensor relaxation can occur until the channel closes. One crucial question is, how are such gating differences achieved between these homologous calcium channels?

Open-state modulation as a potential pharmaceutical target

We recently showed that ω-conotoxin GVIA is a gating modifier that appears to destabilize the N-channel open state by increasing the exit rates from and decreasing the entry rates into both open states (1). Our modeling predicts that this destabilization would result in a maximal 50% inhibition of N-current if it could be separated from the pore-blocking effect of the toxin. Roscovitine, on the other hand, stabilizes open-state occupancy (2,3). Together, these two compounds permit one to modulate the N-channel open state over a wide range to investigate potential physiological and pathophysiological effects, as well as the possible impact of reduced (by ω-conotoxin GVIA-like drugs) or enhanced (by roscovitine-like drugs) N-channel activity on disease.

We thank Dr. Stephen W. Jones for a helpful discussion on an early version of this manuscript.

This work was supported by a grant from the Pennsylvania Department of Health using Tobacco Settlement funds (K.S.E.). The Pennsylvania Department of Health specifically disclaims responsibility for the analyses, interpretations, and conclusions presented here. The authors declare no conflict of interest.

REFERENCES

1. Yarotskyy, V., and K. S. Elmslie. 2008. ω-Conotoxin GVIA alters gating charge movement of N-type (CaV2.2) calcium channels. *J. Neurophysiol.* 101:332–340.
2. Buraei, Z., M. Anghelescu, and K. S. Elmslie. 2005. Slowed N-type calcium channel (CaV2.2) deactivation by the cyclin-dependent kinase inhibitor roscovitine. *Biophys. J.* 89:1681–1691.
3. Buraei, Z., G. Schofield, and K. S. Elmslie. 2007. Roscovitine differentially affects CaV2 and Kv channels by binding to the open state. *Neuropharmacology.* 52:883–894.
4. Cho, S., and S. D. Meriney. 2006. The effects of presynaptic calcium channel modulation by roscovitine on transmitter release at the adult frog neuromuscular junction. *Eur. J. Neurosci.* 23:3200–3208.
5. Yan, Z., P. Chi, J. A. Bibb, T. A. Ryan, and P. Greengard. 2002. Roscovitine: a novel regulator of *P/Q*-type calcium channels and transmitter release in central neurons. *J. Physiol.* 540:761–770.
6. Hess, P., J. B. Lansman, and R. W. Tsien. 1984. Different modes of Ca channel gating behaviour favoured by dihydropyridine Ca agonists and antagonists. *Nature.* 311:538–544.
7. Marks, T. N., and S. W. Jones. 1992. Calcium currents in the A7r5 smooth muscle-derived cell line. An allosteric model for calcium channel activation and dihydropyridine agonist action. *J. Gen. Physiol.* 99:367–390.
8. Artigas, P., G. Ferreira, N. Reyes, G. Brum, and G. Pizarro. 2003. Effects of the enantiomers of BayK 8644 on the charge movement of L-type Ca channels in guinea-pig ventricular myocytes. *J. Membr. Biol.* 193:215–227.
9. Fan, J. S., Y. Yuan, and P. Palade. 2000. Kinetic effects of FPL 64176 on L-type Ca^{2+} channels in cardiac myocytes. *Naunyn Schmiedebergs Arch. Pharmacol.* 361:465–476.
10. Hadley, R. W., and W. J. Lederer. 1992. Comparison of the effects of BAY K 8644 on cardiac Ca^{2+} current and Ca^{2+} channel gating current. *Am. J. Physiol.* 262:H472–H477.
11. McDonough, S. I., Y. Mori, and B. P. Bean. 2005. FPL 64176 modification of CaV1.2 L-type calcium channels: dissociation of effects on ionic current and gating current. *Biophys. J.* 88:211–223.
12. Lee, H. K., and K. S. Elmslie. 1999. Gating of single N-type calcium channels recorded from bullfrog sympathetic neurons. *J. Gen. Physiol.* 113:111–124.
13. Yarotskyy, V., and K. S. Elmslie. 2007. Roscovitine, a cyclin-dependent kinase inhibitor, affects several gating mechanisms to inhibit cardiac L-type (Ca(V)1.2) calcium channels. *Br. J. Pharmacol.* 152:386–395.
14. Buraei, Z., and K. S. Elmslie. 2008. The separation of antagonist from agonist effects of trisubstituted purines on CaV2.2 (N-type) channels. *J. Neurochem.* 105:1450–1461.
15. Bezanilla, F. 2000. The voltage sensor in voltage-dependent ion channels. *Physiol. Rev.* 80:555–592.
16. Dolphin, A. C. 2003. β Subunits of voltage-gated calcium channels. *J. Bioenerg. Biomembr.* 35:599–620.
17. Jones, L. P., C. D. DeMaria, and D. T. Yue. 1999. N-type calcium channel inactivation probed by gating-current analysis. *Biophys. J.* 76:2530–2552.
18. Jones, L. P., P. G. Patil, T. P. Snutch, and D. T. Yue. 1997. G-protein modulation of N-type calcium channel gating current in human embryonic kidney cells (HEK 293). *J. Physiol.* 498:601–610.
19. Zhou, W., and S. W. Jones. 1995. Surface charge and calcium channel saturation in bullfrog sympathetic neurons. *J. Gen. Physiol.* 105: 441–462.
20. Swandulla, D., and C. M. Armstrong. 1989. Calcium channel block by cadmium in chicken sensory neurons. *Proc. Natl. Acad. Sci. USA.* 86:1736–1740.
21. Llinas, R., I. Z. Steinberg, and K. Walton. 1981. Relationship between presynaptic calcium current and postsynaptic potential in squid giant synapse. *Biophys. J.* 33:323–351.
22. Doering, C. J., and G. W. Zamponi. 2003. Molecular pharmacology of high voltage-activated calcium channels. *J. Bioenerg. Biomembr.* 35:491–505.
23. Hockerman, G. H., B. Z. Peterson, B. D. Johnson, and W. A. Catterall. 1997. Molecular determinants of drug binding and action on L-type calcium channels. *Annu. Rev. Pharmacol. Toxicol.* 37:361–396.